Progress In Electromagnetics Research B, Vol. 19, 427–444, 2010

DIELECTRIC RESONATOR ANTENNA MOUNTED ON A CIRCULAR CYLINDRICAL GROUND PLANE

S. H. Zainud-Deen, H. A. Malhat, and K. H. Awadalla

Faculty of Electronic Engineering
Menoufia University
Egypt

Abstract—In this paper, the radiation characteristics of the single-element cylindrical dielectric resonator antenna mounted on the surface of a metallic hollow circular cylindrical structure is investigated. The effect of the radius of curvature on the return loss, input impedance, standing wave ratio, and radiation pattern is explored. Mutual coupling between two identical cylindrical dielectric resonator antennas on a cylindrical structure in different configurations is determined. To reduce the mutual coupling between the two antennas, the surface of the cylinderical ground plane is defected by cutting slots, or inserting quarter wavelength grooves between the two antennas. The finite element method and the finite integration technique are used to calculate the radiation characteristics of the antenna.

1. INTRODUCTION

Dielectric resonator antennas (DRAs) have been widely discussed since it was introduced by Long et al. [1] in 1983. Before that, dielectric resonators were used for filter applications in microwave circuits [2]. In the last decade, dielectric resonator antennas (DRAs) have attracted broad attention in many applications due to their many attractive features in terms of high radiation efficiency, wide bandwidth, light weight, small size and low profile [3–6]. DRAs were considered as better alternative solution to other conventional antenna types for both mobile handset and wireless communication applications. Different shapes of DRAs such as cylindrical, hemispherical, elliptical, pyramidal, rectangular, and triangular have been presented in the literature. Feeding mechanisms that are generally used to excite the DRA include a coaxial probe, a microstrip line coupled to a narrow

Corresponding author: S. H. Zainud-Deen (anssaber@yahoo.com).

slot, or a narrow slot excited by a coplanar waveguide. A comparison between the DRA and the microstrip antenna was presented in [7]. This comparison shows that the DRA can be a more-efficient radiator than the microstrip antenna, can achieve wider-frequency bandwidth, and can have better power-handling capability. The DRA is very small in size, compared to a microstrip antenna, and it is predicted to be a good candidate for an array element.

Most of the work on DRA theory and technology has concentrated on DRA on planar surfaces [8]. However, the situation of DRA on a cylindrical surface is a basic one in many important practical problems. But, to the best of our knowledge, the most interesting case of DRA on cylindrical surface has not been considered. Also, antennas on cylindrical structures play considerable roles in modern communication systems such as spatial domain multiple access (SDMA), smart antennas, beam-steering array antennas and aerospace applications. The surface on which the antenna elements are mounted often affects the radiation properties of the antenna and it is important to be able to predict such variation.

In this paper, the radiation characteristics of the single-element DRA, as well as the two-element array mounted on a cylindrical surface, such as input impedance, return loss, gain, radiation pattern and mutual coupling between DRAs are investigated. A metal hollow circular cylinder, of length L, and radius R is used as the supporting ground for the DRA. The paper is organized as follows. In Section 2, the finite element method and the finite integration technique are explained. As they are used to analyze the problem. In Section 3, the radiation characteristics of a single-element DRA mounted on the surface of a metallic hollow circular cylindrical structure are illustrated. The mutual coupling between two identical DRAs on a circular cylinder is studied as a function of frequency and the distance separating the two antennas in Section 4. Two orientations of DRAs are considered: E-plane coupling and H-plane coupling. Section 5 explains the effect of defected ground structure on the mutual coupling between two identical elements on the cylindrical structure. Finally, Section 6 summarizes the results of investigations conducted in this work.

2. METHODS OF SOLUTION

The finite element method (FEM) is used to calculate the radiation characteristics of the antennas. The results are compared with that calculated by the finite integration technique (FIT). The finite element method is one of the most popular numerical techniques to solve a wide range of problems in applied science and engineering [9, 10]. In

FEM, the region under consideration is discretized by finite elements, a variation of the unknown is assumed within each element, and the element response matrices are then found. Finally, the element response matrices are assembled to obtain the response matrix of the problem domain. The final system of equations is determined as required. In the finite element method, the radiation boundaries are used to simulate open problems that allow waves to radiate infinitely into space. The waves are observed at the radiation boundary surface. More details about the finite element method can be found in [11].

The finite integration technique was first proposed by Weiland in 1977 [12]. FIT was applied to the full set of Maxwell's equations in integral form. FIT describes Maxwell's equations on a grid space, maintaining properties such as energy conservation, and then forms the specific differential equations, such as the Poisson or wave equations. More details about the FIT can be found in [13].

3. SINGLE-ELEMENT CDRA MOUNTED ON A CIRCULAR CYLINDRICAL STRUCTURE

A single-element cylindrical dielectric resonator antenna (CDRA) mounted on a hollow circular cylindrical ground plane is shown in Fig. 1. A cylindrical dielectric resonator antenna with dielectric constant ε_r 12 is used. It has radius, "a", of 4.2 mm and a height, "b", of 3 mm. A coaxial probe with radius of 0.2 mm excites the antenna. The probe is located off the center by df = 3.5 mm with a height, "h", of 2.4 mm. The CDRA is designed to operate around 10 GHz. However, the resonant frequency may alter due to different shapes of the cylindrical ground planes. The length of the circular ground

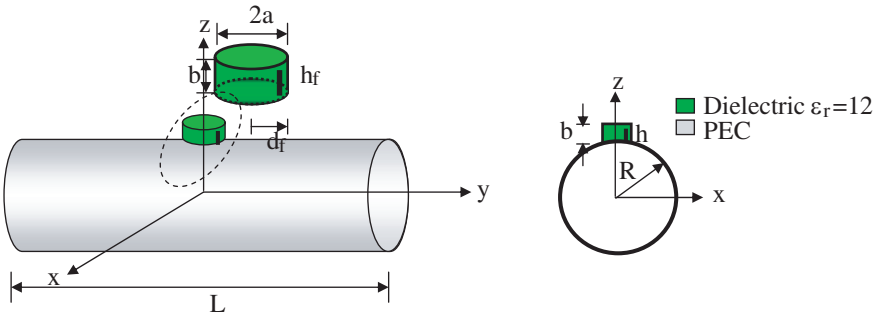

(a) 3-D view (b) 2-D view

Figure 1. The construction of cylindrical dielectric resonator antenna over a hollow circular cylindrical ground plane.

cylinder, "L", is 100 mm. The thickness of the cylindrical conductor shell is 0.6 mm. Without loss of generality, the same CDRA depicted in Fig. 1 is used in all examples to follow. The validity of the FEM (present method) is demonstrated by comparison with published data for CDRA on a planar surface. The results in [14] and the simulated

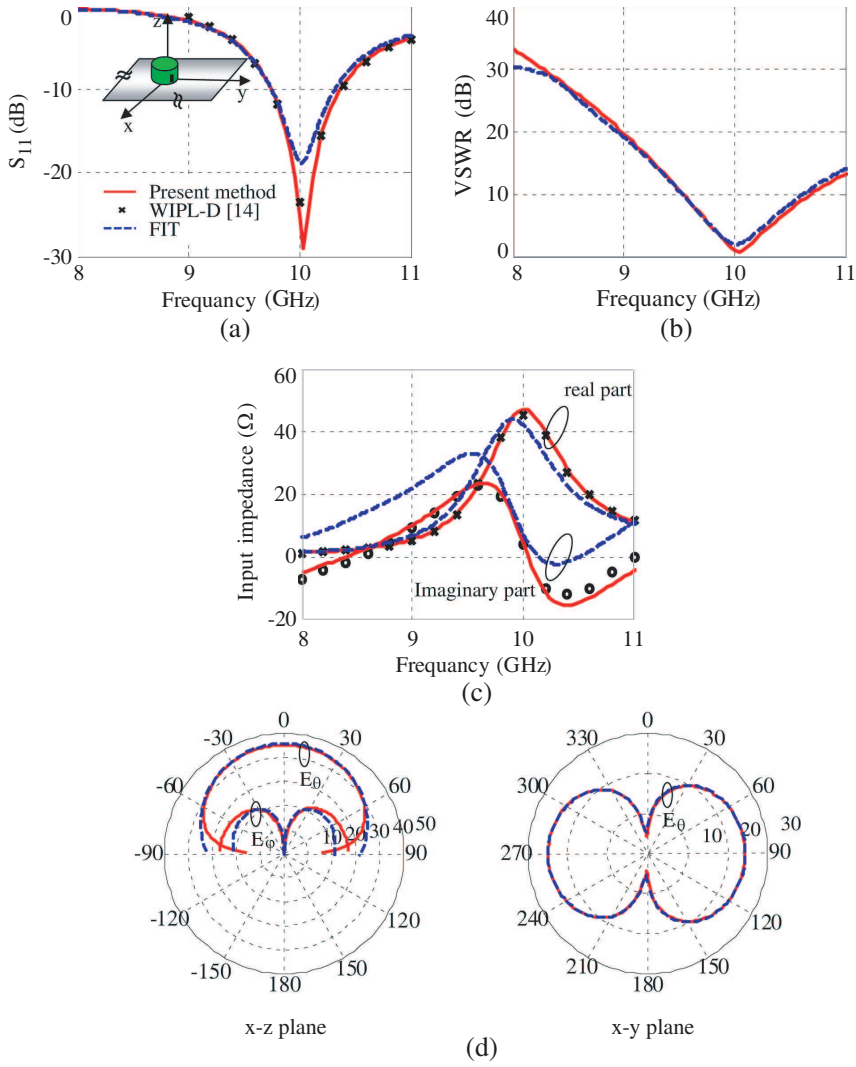

Figure 2. The characteristics of the CDRA on an infinite planar ground plane. (a) The return loss (dB). (b) The VSWR (dB). (c) Input impedance. (Ω). (d) The radiation pattern at 10 GHz.

return loss, S_{11}, voltage standing wave ratio (VSWR), and the input impedance versus the frequency for the CDRA mounted on an infinite planar ground plane are shown in Fig. 2. For comparison the simulation results obtained using the present method, and the results obtained

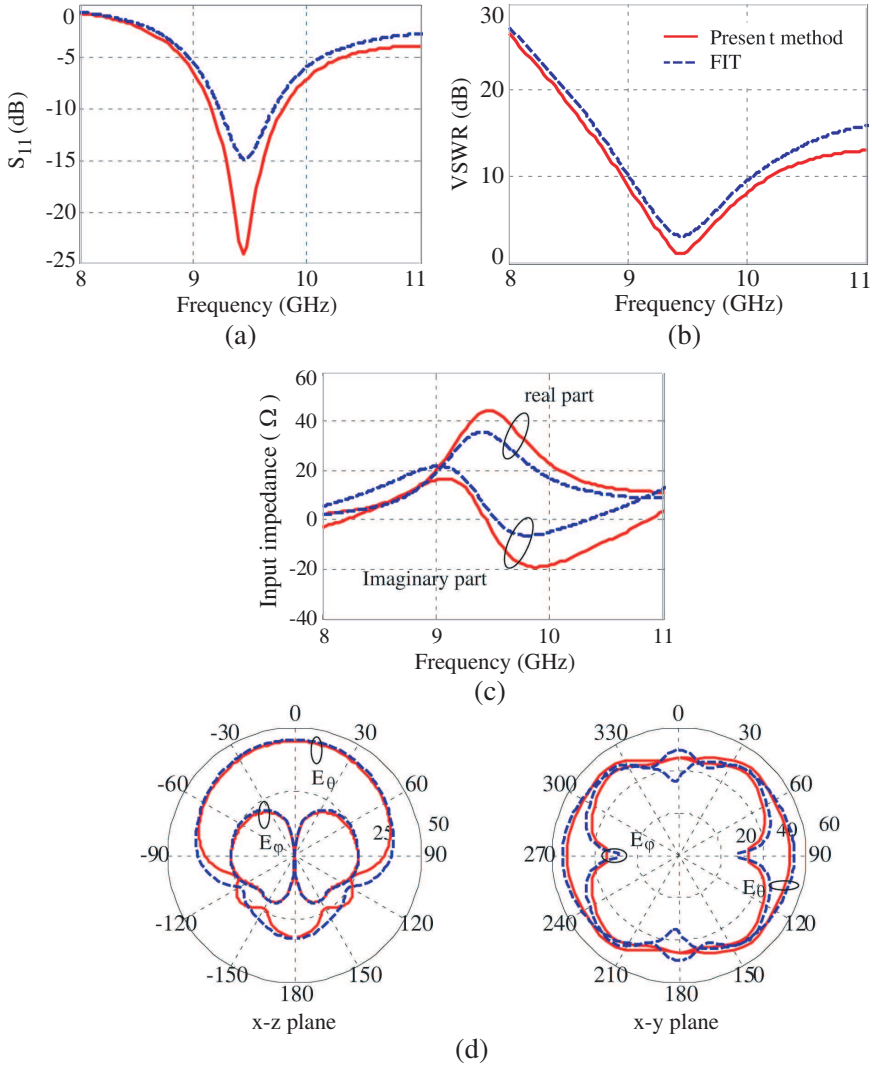

Figure 3. The characteristics of the CDRA on circular cylindrical ground plane with radius $R = 15\,\text{mm}$. (a) The return loss (dB). (b) The VSWR (dB). (c) Input impedance (Ω). (d) The radiation pattern at 9.44 GHz.

using FIT are shown together. The agreement between calculations based on the FEM and published data in [14] is very good. From the figure, it seems that the FIT method according to our implementation is not as good as the other two methods. Other numerical examples are also presented to show the effects of cylinder radius, R, on the

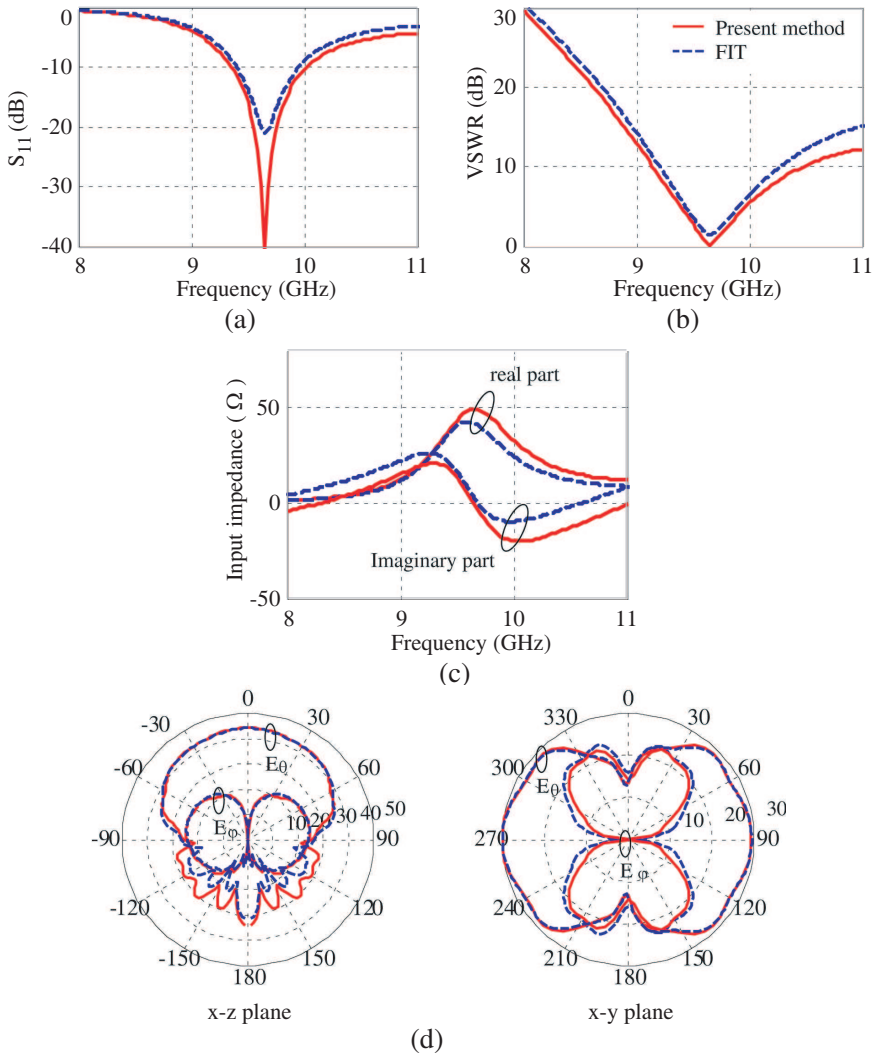

Figure 4. The characteristics of the CDRA on circular cylindrical ground plane with radius $R = 50\,\text{mm}$. (a) The return loss (dB). (b) The VSWR (dB). (c) Input impedance (Ω). (d) The radiation pattern at 9.65 GHz.

radiation characteristics. Figs. 3 to 5 plot the magnitude of S_{11}, VSWR, and the input impedance versus the frequency for cylinders with radiuses $R = 15$, 50 and 100 mm while keeping the rest of the antenna dimensions fixed. Also, the radiation patterns in different planes at frequencies $f = 9.44$, 9.65, and 9.71 GHz are included.

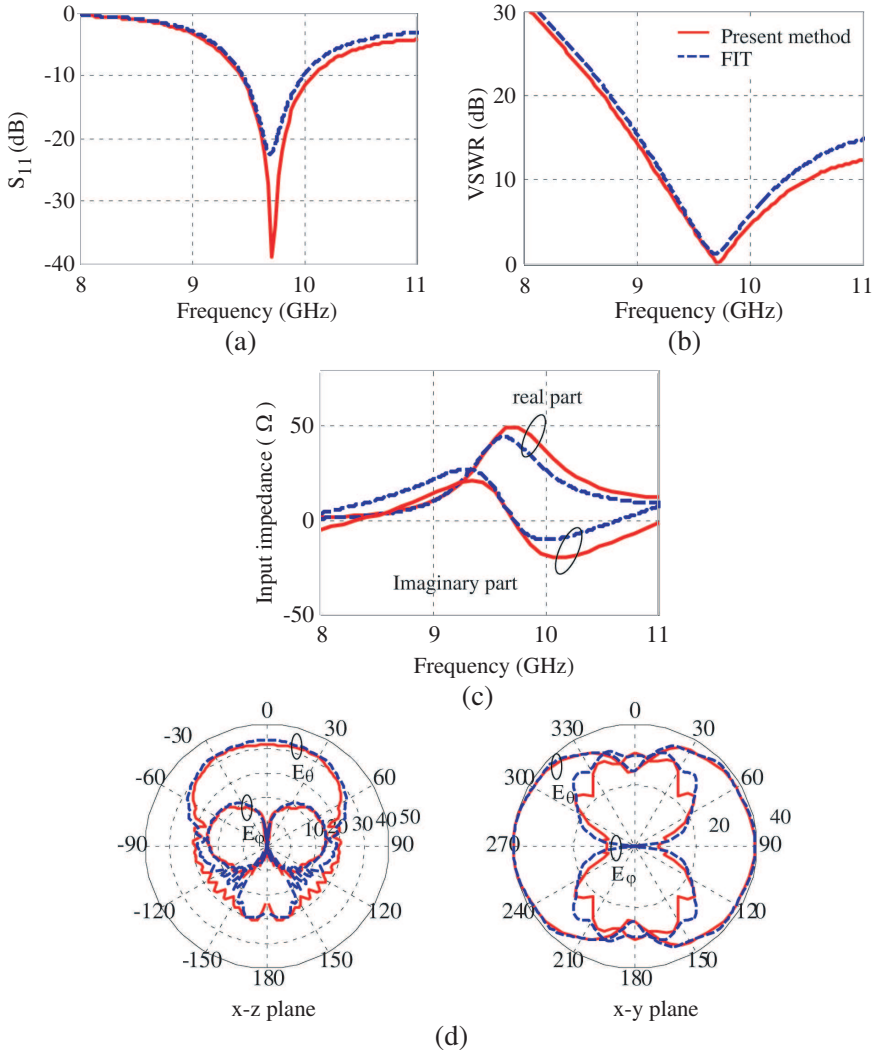

Figure 5. The characteristics of the CDRA on circular cylindrical ground plane with radius $R = 100$ mm. (a) The return loss (dB). (b) The VSWR (dB). (c) Input impedance (Ω). (d) The radiation pattern at 9.71 GHz.

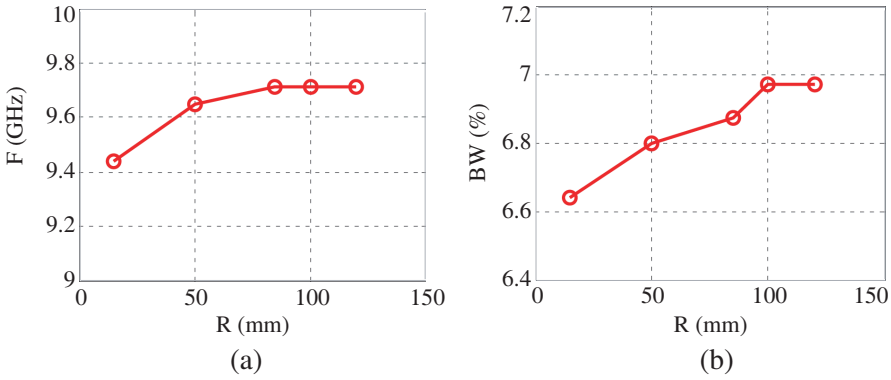

Figure 6. The variation of the characteristics of a single DRA element mounted on a cylindrical ground plane. (a) The resonance frequency versus the ground plane radius R. (b) The impedance bandwidth versus the ground plane radius R.

Figures 6(a) and (b) shows the resonance frequency and the impedance bandwidth variation against the radius of curvature R of the cylindrical ground plane respectively. From these results, it can be seen that the resonance frequency increases with increasing the radius of curvature, R then it remain constant at higher values of R. Also, the impedance bandwidth increases slightly when the radius of the curvature, R, increases. Based on a -10 dB return loss, 6.64% impedance bandwidth in the frequency range of 9.17–9.8 GHz is obtained for the cylinder radius $R = 15$ mm and 6.97% (9.41–10.09 GHz) bandwidth on a cylinder radius $R = 100$ mm. The same CDRA structure, if placed on a planar ground plane, can achieve a -10 dB impedance bandwidth of 6.169% (9.74–10.36 GHz). It is reasonable that when the radius increases, the radiation characteristics approach those of the planar case. The difference between the planar infinite ground plane case and the cylinderical ground plane case,is that when the radius of curvature increases to infinity, the cylinderical ground will be semi-infinite as the length of the cylinderical ground plane remains constant. Thus, there are differences in the resonance frequencies and the radiation characteristics than the infinite planar ground plane.

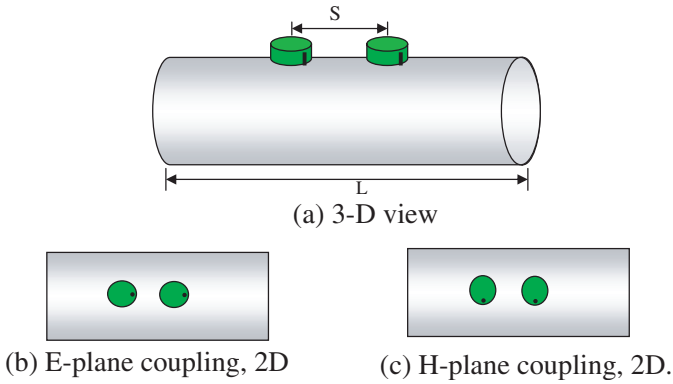

Figure 7. The construction of two identical CDRA over a hollow circular cylindrical ground plane in E-plane and H-plane.

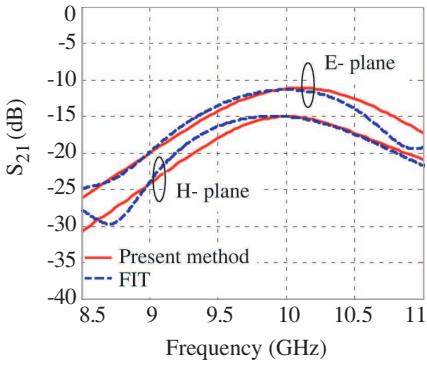

Figure 8. Mutual coupling coefficient (S_{21}) versus frequency for the E-plane coupling and H-plane coupling at $S = 15.789$ mm. The antenna parameters are the same as given in Fig. 1.

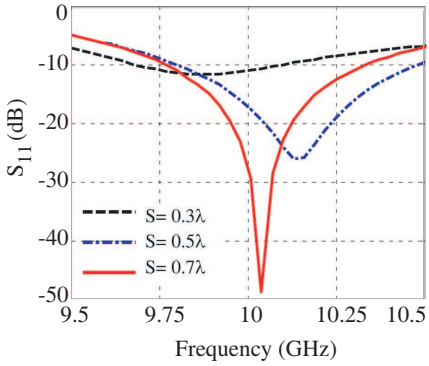

Figure 9. The return loss coefficient (S_{11}) versus frequency for the E-plane coupling plane coupling at $f = 10$ GHz. The antenna parameters are the same as given in Fig. 2.

4. MUTUAL COUPLING BETWEEN TWO IDENTICAL CDRAS MOUNTED ON A CIRCULAR CYLINDER STRUCTURE

The mutual coupling or isolation between closely packed antenna elements is important in a number of applications. These include systems relying on array antennas and more recently multiple input multiple output (MIMO) wireless communication systems which

rely on multiple antennas to offer increase in capacity without the need for additional power or spectrum, compared to conventional systems. Mutual coupling causes some consequences on the antenna's characteristics including modification of the radiation pattern, input impedance, gain and efficiency. Mutual coupling between DRAs have been studied in the past in [15, 16]. Fig. 7 shows the construction of two identical CDRA over hollow circular cylindrical ground plane. Fig. 8 shows the magnitude of the mutual coupling coefficient, S_{21}, as function of frequency when cylinder radius is $R = 15\,\text{mm}$ and separation between element centers $S = 15.789\,\text{mm}$. The figure includes the results for E-plane coupling and H-plane coupling. Fig. 9 shows the magnitude of the return loss, S_{11}, for various antenna separations, "S", versus the frequency. In Fig. 10, the magnitude of S_{21} is plotted as a function of separation, in wavelength, between the two CDRAs for both E-plane coupling and H-plane coupling at $f = 10\,\text{GHz}$. The magnitude of S_{21} as a function of separation, in wavelength, between the two CDRAs for both E-plane coupling and H-plane coupling for various cylinder radii $R = 15$, 50, and 100 mm respectively are plotted in Fig. 11. The coupling decreases faster for the H-plane configuration than for the E-plane with increasing separation between them because of stronger surface waves in the E-plane case. Fig. 12 shows the variation of the mutual coupling and

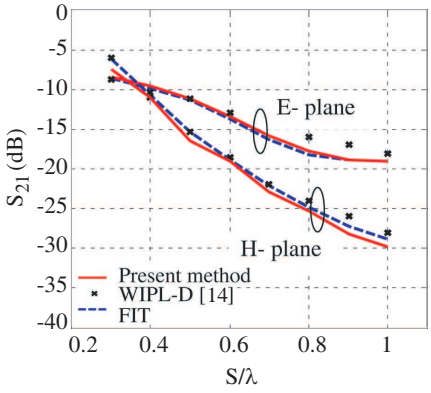

Figure 10. Mutual coupling coefficient (S_{21}) versus frequency for the E-plane coupling and H-plane coupling at $f = 10\,\text{GHz}$. The antenna parameters are the same as given in Fig. 2.

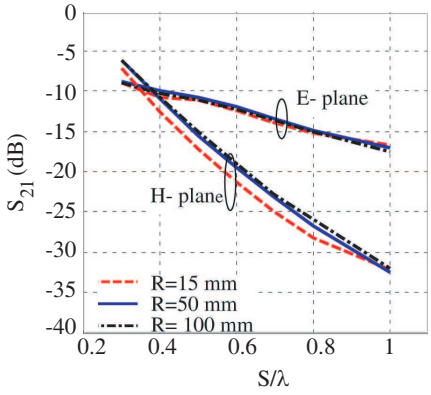

Figure 11. Mutual coupling coefficient (S_{21}) versus separation in wavelength for the E-plane coupling and H-plane coupling at $f = 9.5\,\text{GHz}$.

return loss at the resonance frequency versus the radius of curvature, R. The mutual coupling is decreased with increasing the radius of curvature to some limit ($R = 85\,\text{mm}$) then return to increasing after that. The radiation patterns for the coupled antennas, CDRAs, in different orientations using the same input voltage excitations with $R = 15\,\text{mm}$ at $f = 9.5\,\text{GHz}$ is plotted in Fig. 13. The gain of the two-element DRA array is increased over that of a single element.

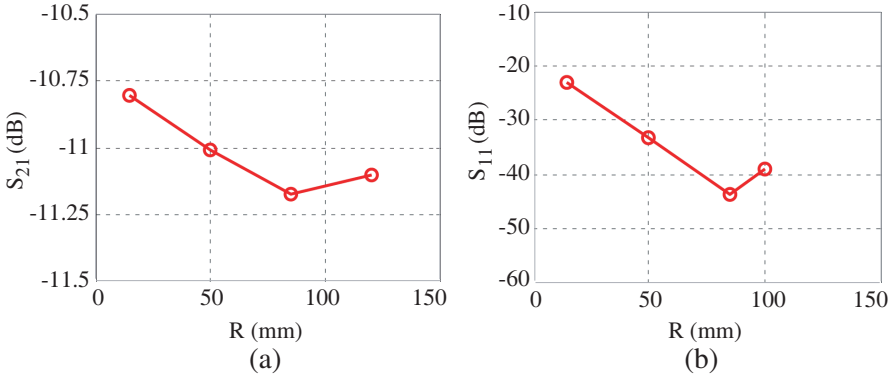

Figure 12. The variation of the characteristics of two-element DRA's elements mounted on a cylindrical ground plane. (a) The maximum mutual coupling versus the ground plane radius R. (b) The minimum return loss versus the ground plane radius R.

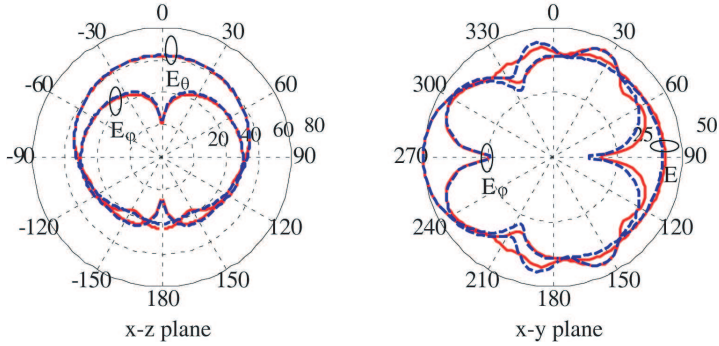

Figure 13. The radiation pattern of two DRAs on cylindrical ground planes of radius 15 mm at 9.5 GHz.

5. CDRAS WITH DEFECTED GROUND CYLINDRICAL STRUCTURE

Achieving low mutual coupling between closely-packed antenna elements is difficult to achieve and has been well studied. Researchers have found that mushroom-like electromagnetic band-gap (EBG) structures are able to suppress surface wave propagation [17, 18], and thus reduce mutual coupling between radiating elements. Additionally researchers have found that the defected ground structures (DGS) are also able to provide a band stop effect due to the combination of inductance and capacitance [19–21]. Fig. 14 shows the construction of two identical CDRA over a hollow circular cylindrical shape with defected ground plane structure (DGS). The DGS is composed of cutting slots in the cylinder wall. The axis of the slot is perpendicular to the cylinder axis. The slot radial length L_s, width W_s, depth H_s, and the slots separation d_s. The dimensions of the slot are designed for their stop-band around 9.5 GHz.

The mutual coupling coefficient S_{21} between two identical CDRAs (with dimensions as in Fig. 1) versus frequency for one slot, two slots and three slots is shown in Fig. 15. The dimensions of the slots are optimized using the genetic algorithm (GA) for minimum coupling coefficient at 9.5 GHz. The optimized dimensions are $L_s = 0.5\lambda$, $W_s = 0.01\lambda$, $H_s = 0$, $d_s = 0.05\lambda$, $S = 0.5\lambda$, and $R = 15$ mm respectively. $H_s = 0$ means that the slots are made as openings in the sheet forming the hollow cylinder. The results are compared with that calculated with a hollow nonslotted conventional cylindrical ground plane. It is observed that, the isolation of the defected ground plane provides a significant improvement of isolation of 14.48 dB for one slot, 17.2 dB for two slots and 15.12 dB for three slots at 9.5 GHz when using the present method. Fig. 16 shows the radiation patterns in different planes for one slot, two slots, and three slots at 9.5 GHz. Little effect has taken place on the radiation pattern for different numbers of slots. It is observed that two slots are enough to give good isolation.

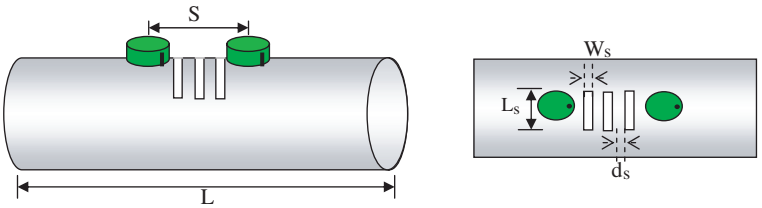

Figure 14. The construction of two identical CDRA over a hollow circular cylindrical shape with defected ground plane structure.

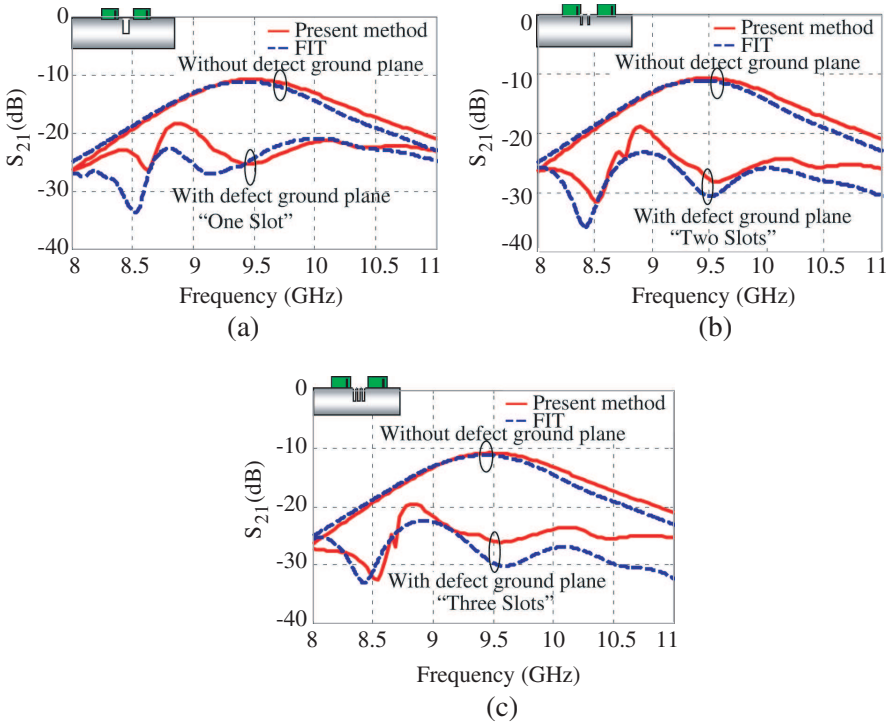

Figure 15. The mutual coupling coefficient S_{21} between two identical CDRA's versus frequency. (a) One slot. (b) Two slots. (c) Three slots.

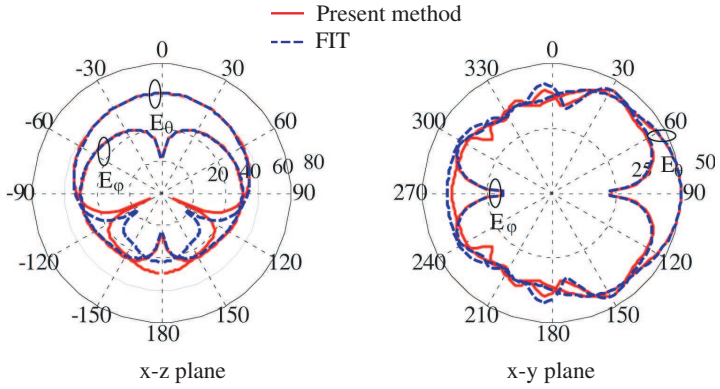

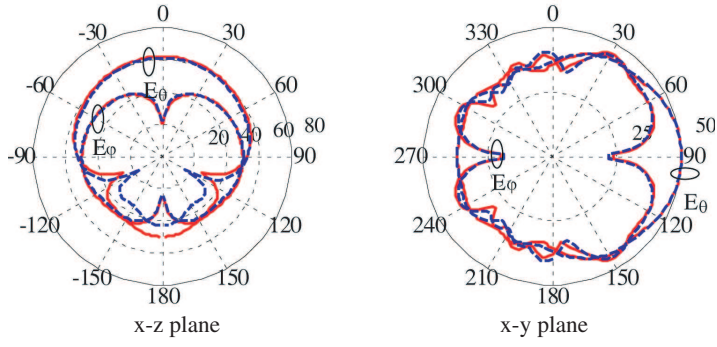

(b)

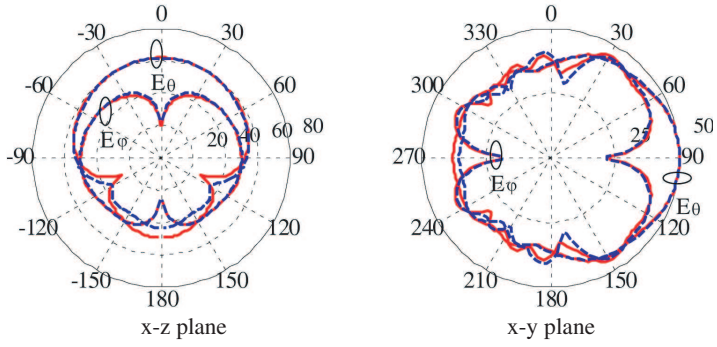

(c)

Figure 16. The radiation pattern for two identical CDRA's with defected ground plane structure at 9.5 GHz. (a) One slot. (b) Two slots. (c) Three slots.

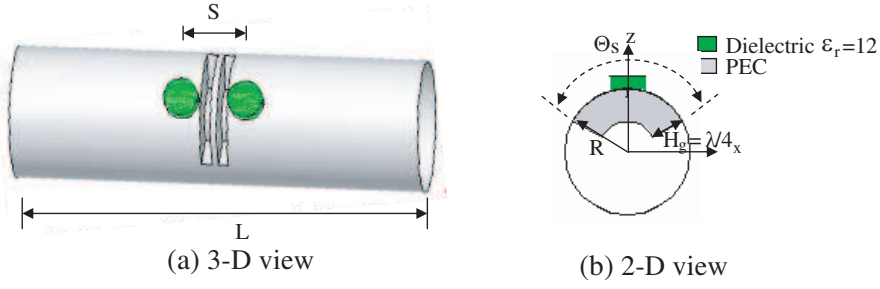

(a) 3-D view (b) 2-D view

Figure 17. The construction of two identical CDRA's over a hollow cylindrical shape with tilted defect cylindrical ground plane.

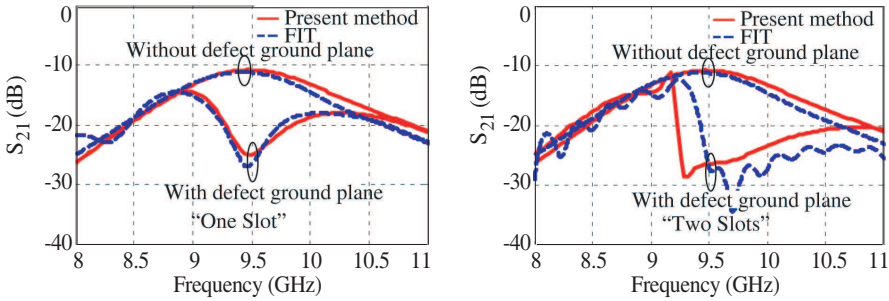

Figure 18. The mutual coupling coefficient, S_{21}, between two identical CDRA's versus frequency. with tilted defected ground plane. (a) One slot. (b) Two slots.

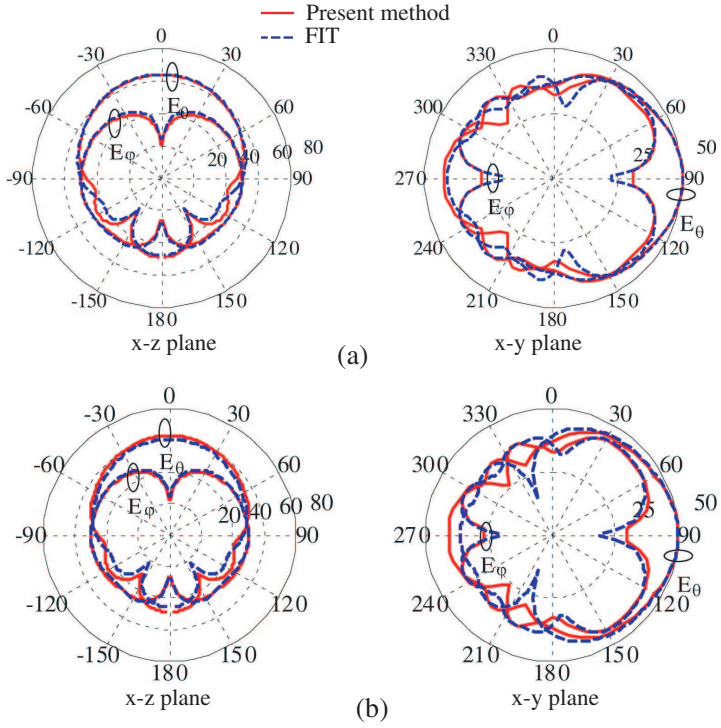

Figure 19. The radiation pattern for two identical CDRA's with tilted defected ground plane structure at 9.5 GHz. (a) One slot. (b) Two slots.

Another shape for cutting slots is shown in Fig. 17. The cutting slot (quarter wavelength groove) is tilted and it is boxed with its bottom is made cylindrical with the same axis of the original ground cylinder. The depth $H_s = \lambda/4$ and $\theta_s = 60.3^\circ$ with $W_s = 0.02\lambda$, and $d_s = 0.1\lambda$ at the center frequency 9.5 GHz. Fig. 18 shows S_{21} between the two DRAs with tilted defected ground plane versus frequency for one slot and two slots. The separation $S = 15.789$ mm, cylinder radius $R = 15$ mm. An isolation of 14.13 dB for one slot and 15.6 dB for two slots over the hollow nonslotted conventional ground plane is obtained. Using the present method, the effect of two slots is again better in isolation. However, it becomes clear that there is no need to box the slots. The radiation patterns at 9.5 GHz and $R = 15$ mm for one slot and two slots in different planes are plotted in Fig. 19. The shape of the radiation pattern is almost the same.

6. CONCLUSION

This paper presents the simulated results for the radiation characteristics of the single-element CDRA mounted on the surface of a metallic hollow circular cylindrical structure. Two methods of solution are used, the FEM and FIT. The results indicate that the resonance frequency of the antenna, input impedance and the radiation pattern are changed by increasing the radius of the cylindrical structure. The mutual coupling between two identical CDRA is investigated in E-plane coupling and H-plane coupling. The coupling decreases faster for the H-plane coupling than for the E-plane coupling. The mutual coupling coefficient S_{21} is quite stable with changing the radius of the cylinder. The surface of the cylinder is defected by using slots to decrease the mutual coupling between the two CDRAs. The S_{21} is decreased by 14.48 dB for one slot, 17.2 dB for two slots and 15.12 dB for three slots at the center frequency $f = 9.5$ GHz. Thus, it has been shown that two slots is an optimum choice, and there is no need to box the slots because boxing gives no improvement relative to the free slots.

REFERENCES

1. Long, S. A., M. W. McAllister, and L. C. Shen, "The resonant cylindrical dielectric cavity antenna," *IEEE Transactions on Antennas and Propagation*, Vol. 31, No. 5, 406–412, May 1983.
2. Kajfez, D. and P. Guillon, *Dielectric Resonators*, Artech House, Norwood, MA, 1986.
3. Luk, K. M. and K. W. Leung, *Dielectric Resonator Antenna*, Research Studies Press, Hertfordshire, UK, 2003.

4. Chang, T.-H. and J.-F. Kiang, "Sectorial-beam dielectric resonator antenna for WiMAX with bent ground plane," *IEEE Transactions on Antennas and Propagation*, Vol. 57, No. 2, 563–572, February 2009.
5. Guha, D. and Y. M. M. Antar, "Four-element cylindrical dielectric resonator antenna for wideband monopole-like radiation," *IEEE Transactions on Antennas and Propagation*, Vol. 54, No. 9, 2657–2662, September 2006.
6. Hady, L. K., D. Kajfez, and A. A. Kishk, "Triple mode use of a single dielectric resonator," *IEEE Transactions on Antennas and Propagation*, Vol. 57, No. 5, 1328–1335, May 2009.
7. Lai, Q., G. Almpanis, C. Fumeaux, H. Benedickter, and R. Vahldieck, "Comparison of the radiation efficiency for the dielectric resonator antenna and the microstrip antenna at Ka band," *IEEE Transactions on Antennas and Propagation*, Vol. 56, No. 11, 3589–592, November 2008.
8. Yang, L., H.-C. Yang, and C.-L. Ruan, "A novel wideband dielectric resonator antenna," *Journal of Electromagnetic Waves and Applications*, Vol. 22, No. 11–12, 1499–1507, 2008.
9. Dong, X. and T. An, "A new FEM approach for open boundary Laplace's problem," *IEEE Trans. Microw. Theory Tech.*, Vol. 44, No. 1, 157–160, January 1996.
10. Zhou, X. and G. W. Pan, "Application of physical spline finite element method (PSFEM) to full wave analysis of waveguide," *Progress In Electromagnetics Research*, PIER 60, 19–41, 2006.
11. Harscher, P., S. Amari, and R. Vahldieck, "A fast-element-based field optimizer using analytically calculated gradients," *IEEE Trans. Microw. Theory Tech.*, Vol. 50, No. 2, 433–439, February 2002.
12. Weiland, T., "A discretization method for the solution of Maxwell's equations for six-component fields," *Electromagnetics and Communications AEÜ*, Vol. 31, No. 3, 116–120, March 1977.
13. Clemens, M. and T. Weiland, "Discrete electromagnetism with the finite integration technique," *Progress In Electromagnetics Research*, PIER 32, 65–87, 2001.
14. Chair, R., A. A. Kishk, and K. F. Lee, "Comparative study on the mutual coupling between different sized cylindrical dielectric resonators antennas and circular microstrip patch antennas," *IEEE Transactions on Antennas and Propagation*, Vol. 53, No. 3, 1011–1019, March 2005.
15. Khayat, M. A. and J. T. A. Williams, "Mutual coupling

between cylindrical probe-fed dielectric resonator antennas," *IEEE Antennas and Wireless Propagation Letters*, Vol. 1, 8–9, January 2002.

16. Kwai-Man, L., L. Wai-Kee, and L. Kwok-Wa, "Mutual impedance of hemispherical dielectric resonator antennas," *IEEE Transactions on Antennas and Propagation*, Vol. 42, No. 12, 1652–1654, December 1994.
17. El-Deen, E., S. H. Zainud-Deen, H. A. Sharshar, and M. A. Binyamin, "The effect of the ground plane shape on the characteristics of rectangular dielectric resonator antennas," *IEEE APS/URSI/AMEREM 2006 Symposium*, Albuquerque, New Mexico, USA, July 2006.
18. El-Deen, E., "Analysis of electromagnetic waves in the time domain," MSc. Thesis, Faculty of Electronic Engineering, Menoufia University, Egypt, 2006.
19. Zainud-Deen, S. H., M. E. S. Badr, and E. El-Deen, "Microstrip antenna with defected ground plane structure as a sensor for landmines detection," *Progress In Electromagnetics Research B*, Vol. 4, 27–39, 2008.
20. Weng, L. H., Y. C. Guo, X. W. Shi, and X. Q. Chen, "An overview on defected ground structure," *Progress In Electromagnetics Research B*, Vol. 7, 173–189, 2008.
21. Zainud-Deen, S. H., M. E. Badr, E. El-Deen, K. H. Awadalla, and H. A. Sharshar, "Microstrip antenna with corrugated ground plane surface as a sensor for landmines detection," *Progress In Electromagnetics Research B*, Vol. 2, 259–278, 2008.